

Interactive Humanoid: Online Full-Body Motion Reaction Synthesis with Social Affordance Canonicalization and Forecasting

Yunze Liu^{1,3}, Changxi Chen¹, Li Yi^{1,2,3},

¹ Tsinghua University, ² Shanghai Artificial Intelligence Laboratory, ³ Shanghai Qi Zhi Institute

Abstract

We focus on the human-humanoid interaction task optionally with an object. We propose a new task named online full-body motion reaction synthesis, which generates humanoid reactions based on the human actor’s motions. The previous work only focuses on human interaction without objects and generates body reactions without hand. Besides, they also do not consider the task as an online setting, which means the inability to observe information beyond the current moment in practical situations. To support this task, we construct two datasets named HHI and CoChair and propose a unified method. Specifically, we propose to construct a social affordance representation. We first select a social affordance carrier and use $SE(3)$ -Equivariant Neural Networks to learn the local frame for the carrier, then we canonicalize the social affordance. Besides, we propose a social affordance forecasting scheme to enable the reactor to predict based on the imagined future. Experiments demonstrate that our approach can effectively generate high-quality reactions on HHI and CoChair. Furthermore, we also validate our method on existing human interaction datasets Interhuman and Chi3D. Website: <https://yunzeliu.github.io/iHuman/>

1. Introduction

In various applications including VR/AR, games, and human-robot interaction, there is a strong demand for generating reactive humanoid characters or robots based on the actions of human actors. Such a reaction needs to occur in real-time, dynamically responding to the movements of the human actor. Furthermore, in many cases, these interactions involve objects (e.g., a human and a humanoid collaboratively carrying a chair) and call for an emphasis on the precise movements of humanoid hands in addition to the overall body motion. Addressing the challenge of synthesizing humanoid¹ reactions in these contexts can significantly enhance the social experience of humans interacting with humanoids and bring a whole new entertainment.

¹In this paper, we use *human* to denote real people initiating interactions and *humanoid* to indicate the virtual character reacting in response.

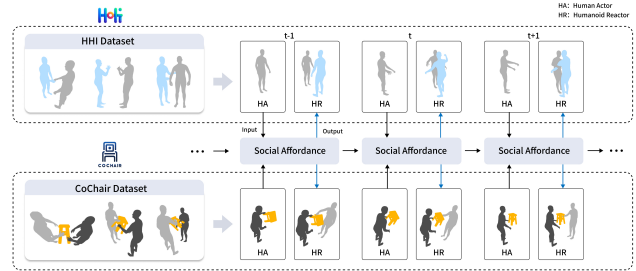


Figure 1. We propose a new task named online full-body motion reaction synthesis optionally with an object. Left: we construct two datasets HHI and CoChair to support the task. Right: we propose Social Affordance Canonicalization and Forecasting technique to generate realistic reactions and establish benchmarks.

Previous research on humanoid motion synthesis has mainly focused on single humanoid movements [4, 15, 18, 22, 40, 49, 56] or interactions with objects [13, 51, 54, 55, 57, 59]. Some recent studies [30, 49], have explored the synthesis of social interactions between two humanoids. However, these studies have limitations. Firstly, they primarily focus on the offline generation between two humanoids, which is not suitable for the asymmetric reaction synthesis setting where the humanoid continuously responds to the dynamic human actor in an online manner. Secondly, they overlook the fact that humans often interact through objects. Thirdly, these works do not consider synthesizing full-body motions involving both body and hand motions, which are crucial for various interactions such as handshakes or collaborations. Therefore, synthesizing full-body humanoid reactions online considering both human actors and the possible objects goes beyond the scope of existing works, presenting three major challenges: 1) representing complex motions of a human actor and optionally an object, 2) interpreting the human actor’s intentions for prompt reactions by the humanoid, and 3) supporting detailed reactions involving both coarse-grained body movements and fine-grained hand movements.

To address the challenges mentioned, we draw inspiration from affordance learning. Our approach involves encoding the motion of the human actor (possibly with an object) as a social affordance representation, capturing sup-

ported and expected social interactions at both the body and hand levels. Subsequently, we learn the humanoid’s reaction based on the social affordance representation. To simplify the distribution of social affordance and facilitate learning, we employ a canonicalization technique. Furthermore, we introduce an online social affordance forecasting scheme to enable the humanoid to react promptly.

Specifically, our method handles a sequential input data stream comprising the human actor’s pose at each time step. When objects are involved, the input also includes a stream of 6D-transforming 3D shapes. To unify the input with and without objects, we introduce the concept of “affordance carrier”, which can be either the real object in human-object-humanoid interactions or just the reactor in a rest state in human-humanoid interaction. Centering around the affordance carrier, we propose a social affordance representation encompassing the actor’s motion, the carrier’s dynamic geometry, and the actor-carrier relationship up until each time step. And then we learn to predict the humanoid’s online reaction through a 4D motion transformer. However, we find directly predicting the reaction based on the social affordance representation not satisfactory enough for two reasons. First, the actor’s motion exhibits diverse patterns, complicating the social affordance and increasing the learning difficulty. To address this, we observe that the patterns within the actor’s motion become more compact when viewed from the carrier’s local coordinate system. Therefore, we present a social affordance canonicalization strategy enabled by equivariant local frame learning. Second, the humanoid reactor can only access present and past observations, limiting its social affordance to short-sighted information and hindering prompt reactions. To overcome this, we propose a social affordance forecasting scheme to enable the reactor to predict based on the imagined future.

To validate the effectiveness of our design and also to address the lack of large-scale full-body reaction-synthesis benchmarks, we have gathered two large-scale full-body social interaction datasets named HHI and CoChair. HHI covers a diverse range of human-human interactions with a clear actor and reactor while CoChair focuses on human-object-human interaction. Our method consistently outperforms previous methods in all metrics. We also validate our method on existing datasets Interhuman and Chi3D.

The key contributions of this paper are threefold: i) we propose a new task named online full-body motion reaction synthesis optionally with an object and establish benchmarks; ii) we construct two datasets HHI and CoChair to support the research on full-body reaction synthesis tasks; iii) we propose a unified solution to reaction synthesis with or without objects by social affordance canonicalization and forecasting, significantly outperforming baselines.

2. Related Work

Human Motion Generation. Human motion generation is to generate human motion conditioned on different signals. A line of works[4, 9, 11, 18, 39, 49, 52] propose to generate human motion conditioned on action label. Some works[1, 15, 19, 22, 24, 40, 56] directly generate human motion conditioned on text description. There are also some works[25, 27, 29] that generate human motion conditioned on music and speech. Recently, some works[30, 44, 46, 49] have started to focus the human-human interaction synthesis. [30] propose a new dataset with natural language descriptions and design a diffusion model to generate human-human interaction. However, this method cannot be directly applied to reaction synthesis because it uses a fixed CLIP[41] branch to extract text features. [49] presents a GAN-based Transformer for action-conditioned motion generation. However, it cannot generate full-body motions and cannot handle the presence of objects.

Human Reaction Generation. We focus on motion generation conditioned on another human motion. Human reaction generation is conditioned on the actor’s motion and requires the reactor to provide a reasonable response, which is very important in the fields of VR/AR and humanoid robots. [12] propose a Transformer network with both temporal and spatial attention to generate reactions. [6] propose to predict human intent in Human-Human interactions. However, they are only concerned with the generation of body motions and cannot generate hand motions. At the same time, they only focus on the interaction between humans and cannot generate reasonable reactions in the presence of objects. In addition, reaction synthesis should be in an online setting, meaning that the reactor cannot observe future information, which is also not discussed in previous work. There is no dataset providing full-body human-human interaction and human-object-human interaction with clear actor and reactor, so in this paper, we first construct two datasets and propose a novel method to generate realistic reactions.

Human Motion Prediction Human motion prediction [8, 14, 21, 28, 35, 36, 45, 45, 47, 58] is a traditional task widespread attention. A line of works predicts human motions in an encoding-decoding way [7, 16, 32, 42, 50]. Some works carefully designed loss constraints [3, 20, 26] to generate diversity and realistic human motions. Without multi-stage training,[10] propose a human motion diffusion model to predict human motion in a masked completion fashion. Besides, [51] propose to predict human motion with the object as an HOI sequence and use interaction diffusion and interaction correction to predict the future state of human and object. In this paper, we focus on human-human and human-object-human interactions. We propose to use a motion forecasting module to improve the ability of the reactor, thus relying on both human motion prediction and human-object interaction prediction methods.



Figure 2. We construct two datasets to support the research on reaction synthesis. HHI(left) is the first large-scale whole-body motion reaction dataset with clear action feedback. CoChair(right) is the first large-scale dataset for multi-human and object interaction

3. Datasets

3.1. HHI: Human-Human Interaction

The HHI dataset is a large-scale full-body motion reaction dataset with clear action feedback which includes 30 interactive categories, 10 pairs of human body types, and a total of 5,000 paired interaction sequences. The HHI dataset has three characteristics. The first is *multi-human whole-body interaction* including body and hand interactions which is not supported in previous datasets. We believe hands are essential in multi-human interactions and can convey rich information during handshake, hug, and handover. The second is our dataset can distinguish *distinct actors and reactors*. For example, during handshakes, pointing directions, greetings, handovers, etc., We can identify the initiator of the action, which can help us better define and evaluate this problem. The third is our dataset has a *rich diversity*, which includes the types of interactions and reactions. We not only include 30 types of interactions between two humans but also provide multiple reasonable reactions for the same action by the actor. For example, when someone greets you, you can nod in response, respond with one hand, or respond with both hands. This is also a natural feature that humans possess when reacting, but previous datasets have rarely focused on this point and discussed it.

3.2. CoChair: Human-Object-Human Interaction

CoChair is a large-scale dataset for multi-human and object interaction consisting of 8 different chairs, 5 interaction patterns, and 10 pairs of different skeletons, totaling 3000 sequences. CoChair has two significant characteristics. CoChair is information asymmetry during collaboration. Each action has an actor/initiator (who knows the destination of the carrying) and a reactor (who does not know the destination), which can support our research on the reactor’s behavior patterns. The second is the diversity of carrying patterns. The dataset includes five carrying patterns: one-hand fixed carrying, one-hand mobile carrying, two-hand fixed carrying two-hand mobile carrying, and two-hand flexible carrying.

3.3. Dataset Construction.

Dataset Comparison. HHI is the first large-scale dataset with diverse interactions for whole-body reaction synthesis. It not only provides motion capture of the whole body but also designs interaction with clear initiators. Compared to the challenging free-from interaction provided by Interhuman, our dataset has explicit categories of interactive actions, which facilitates the evaluation of generated results. Compared to datasets such as SBU, K3HI, and Chi3D which fully or partially use image-based methods to estimate human poses, our dataset is completely captured by motion capture devices and meticulously annotated by human experts, which can provide higher-quality motions.

CoChair is the first large-scale dataset for human-object-human collaborative carrying. It not only has clear motion initiators but also diverse object geometries and different carrying patterns. Compared to other datasets, we support a more challenging setting that involves not only human interaction but also the interaction between humans and objects.

Dataset	Object	Full-body	Actor&Reactor	Mocap	Motions	Verbs	Duration
SBU[53]	-	-	-	-	282	8	0.16h
K3HI[5]	-	-	-	-	312	8	0.21h
NTU120[31]	-	-	-	-	739	26	0.47h
You2me[37]	-	-	-	-	42	4	1.4h
Chi3D[17]	-	-	-	✓	373	8	0.41h
InterHuman[30]	-	-	-	✓	6022	5656	6.56h
HHI (Ours)	-	✓	✓	✓	5000	30	5.55h
CoChair (Ours)	✓	✓	✓	✓	3000	5	2.78h

Table 1. **Dataset comparisons.** We compare our iHuman dataset with existing multi-human interaction datasets. **Object** refers to human-object-human interaction. **Whole-body** refers to whole-body motion capture. **Actor&Reactor** refers to whether there is an obvious initiator of the action. **Motions** is the total number of motion clips. **Verbs** is the number of interaction categories. **Duration** refers to the total time of each dataset.

Dataset Collection. We use 12 NOKOV motion capture cameras with 60fps for data collection. The cameras are arranged in a square formation on the ceiling, with four cameras on each side. For the body, each participant has to attach 53 markers. As for the hands, we attached 32 markers to the wrists, finger joints, and fingertips (16 markers per

hand). For tracking objects during interactions, we affix 9 markers to each object. During the interaction, only the actor knows the task and we allow them to decide whether or not to share this information with the reactor. Then the actor decides when to start the carrying process. This ensures the authenticity of the reaction when it responds. The actor will initiate the motion first, and then the reactor will respond accordingly based on instinct and habit.

Dataset annotation. We track 53 markers on the body and 16 markers on each hand. Followed by AMASS[34], we obtain SMPL-X[38] parameters for each frame through optimization. For each object, we mark the position of the attached marker on the scanned CAD model and calculate the transformation matrix.

4. Method

Our goal is to generate motions for the humanoid to interact or collaborate with the human in social scenarios or collaborative tasks, which requires the humanoid to not only understand the human’s intentions and motions but also comprehend the state of the environment or objects. In this Section, we elaborate on the method in detail. We first introduce the concept of social affordance carrier and carrier-centric representation. Then we introduce the social affordance canonicalization technique to simplify the distribution of social affordance and facilitate learning. We also introduce an online social affordance forecasting scheme to enable the humanoid to react promptly. Finally, we show the 4D motion transformer and objective function for the entire framework.

4.1. Social Affordance Carrier

Social affordance carrier refers to the object or humanoid encoding social affordance information. When a human actor interacts with a humanoid, the human actor often comes into contact with the humanoid directly or indirectly. And when there is an object, human actors often come into direct contact with the object. In order to model the direct or potential contact information in the interaction, we need to choose a carrier to simultaneously represent the human actor, the carrier, and the relationship between them. We choose the carrier to be an object or humanoid with which the human actor has potential contact. We denote a sequence with L frames as $\mathbf{s} = [\mathbf{s}^1, \mathbf{s}^2, \dots, \mathbf{s}^L]$, where \mathbf{s}^i consists of human actor \mathbf{h}^i and Carrier \mathbf{c}^i . Carrier refers to the object or the humanoid in the rest pose. Human actor $\mathbf{h}^i \in \mathbb{R}^{J \times D_h}$ is defined by J joints with a D_h -dimensional representation at each joint, which is joint position and its velocity. Carrier $\mathbf{c}^i \in \mathbb{R}^{N \times 3}$ is defined by N object points or humanoid joints with its position. We denote the humanoid reactor sequence as $\mathbf{s}_r = [\mathbf{s}_r^1, \mathbf{s}_r^2, \dots, \mathbf{s}_r^L]$. Given the sequence of human actor and carrier \mathbf{s} , our goal is to predict a reasonable humanoid reactor sequence \mathbf{s}_r .

4.2. Social Affordance Representation

We define the social affordance representation centered on the carrier. Specifically, given a carrier, we encode the human actor motions to obtain a dense human-carrier representation. With this representation, we propose a social affordance representation that contains the motion of the human actor, the carrier’s dynamic geometry, and the actor-carrier relationship up until each time step. Note that the social affordance representation refers to the data stream from the beginning to a certain time step, rather than the representation of a single frame. The advantage of the social affordance representation is that it tightly associates the local region of the carrier with the human actor’s motion, forming a strong representation for network learning.

Carrier-centric actor representation. Given a human actor \mathbf{h}^i and a carrier \mathbf{c}^i at time step i , we first define the carrier-centric actor representation R^i as a collection of point-wise vectors on a set $\{\mathbf{x}_j^i\}_{j=1}^N$ of N points or joints from carrier \mathbf{c} .

$$\mathbf{R}^i(\mathbf{h}^i, \mathbf{c}^i) = \{(\mathbf{x}_j^i, \epsilon_\theta(\mathbf{h}^i))\}_{j=1}^N, \quad (1)$$

where R^i is carrier-centric actor representation, \mathbf{x}_j^i is the position of the point or joints from the carrier at time step i , \mathbf{h}^i is the human actor at time step i and ϵ_θ is the GNN network to encode human actor’s motion to an embedding.

Social Affordance representation. Given the carrier-centric actor representation at each time step, we define the social affordance representation A^i as a collection of $\{\mathbf{R}^t\}_{t=1}^i$ up until each time step.

$$\mathbf{A}^i = \{\mathbf{R}^t\}_{t=1}^i = \{(\mathbf{x}_j^t, \epsilon_\theta(\mathbf{h}_j^t))\}_{j=1}^N\}_{t=1}^i, \quad (2)$$

where A^i refers to the social affordance representation at time step i and R^t refers to carrier-centric actor representation at time step t .

4.3. Social Affordance Canonicalization

Learning Local Frames for Carrier. We believe that a local frame can reflect the geometric information of the carrier and can reflect the contact information between the carrier’s local area and the human actor. Let \mathbf{c} denote the carrier and $\{\mathbf{x}_j\}_{j=1}^N$ as each point or joint. Let H and \mathbf{V} denote per-point invariant scalar features and equivariant vector features of \mathbf{c} , respectively.

We use $\mathbf{c}, H_{in}, \mathbf{V}_{in}$ to denote the carrier, invariant scalar, and equivariant vector features, where H_{in}, \mathbf{V}_{in} are all zeros. We pass the carrier to an Equivariant network that aims to extract invariant and equivariant features, denoted as EquivLayer. Our EquivLayer is adapted from the GVP-GNN layer[23].

$$(H_{out}, \mathbf{V}_{out}) \leftarrow \text{EquivLayer}(\mathbf{c}, H_{in}, \mathbf{V}_{in}). \quad (3)$$

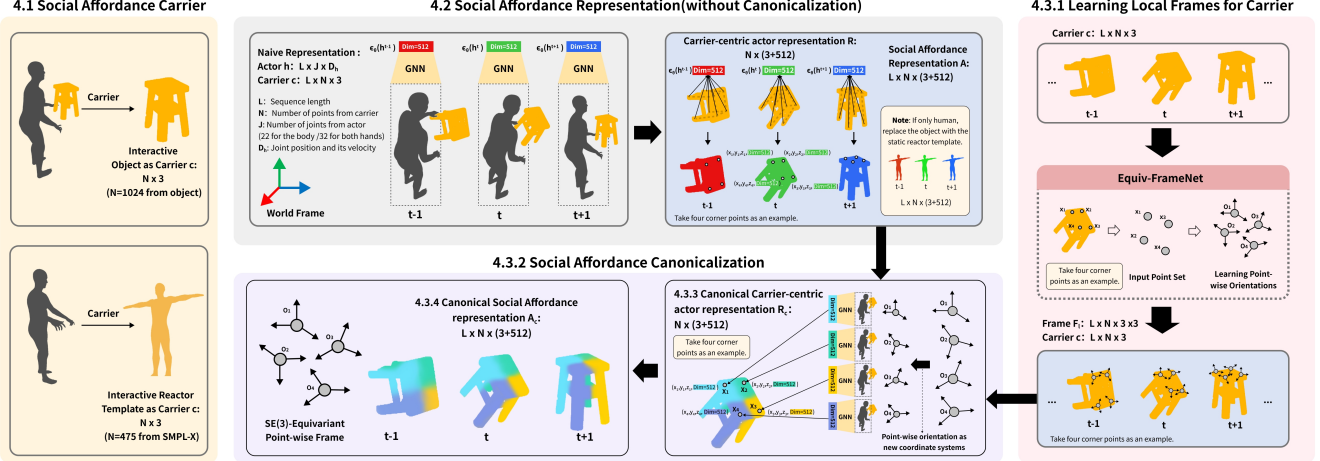


Figure 3. Social Affordance Canonicalization. Given a sequence, we first select a social affordance carrier and build the carrier-centric representation. Then we can compute the social affordance representation. We propose to learn the local frame for carrier and canonicalize social affordance to simplify the distribution. Then a motion encoder and decoder are used to generate reactions.

Since EquivLayer is equivariant at all the layers, and the inputs H_{in}, \mathbf{V}_{in} are invariant and equivariant features, the output $H_{out}, \mathbf{V}_{out}$ of each layer are also invariant and equivariant features, respectively.

To obtain local frames of each point from invariant and equivariant features, we use another set of equivariant networks adapted from the GVP layers[23]. We use FrameNet to denote the network.

$$\mathbf{V}_{out} \leftarrow \text{FrameNet}(H_{out}, \mathbf{V}_{out}), \quad (4)$$

where each frames will be constructed from the equivariant features $\mathbf{V}_{out} = (\mathbf{v}_{out,1}, \dots, \mathbf{v}_{out,N}) (\mathbf{v}_{out,j} \in \mathbb{R}^{2 \times 3})$.

We orthonormalize the two vectors $\mathbf{v}_{out,j,1}, \mathbf{v}_{out,j,2}$ for each point to get $\mathbf{u}_{j,1}, \mathbf{u}_{j,2}$ using the Gram-Schmidt method. Then we get the local frame $\mathbf{F}_l = \{\mathbf{F}_j\}_{j=1}^N = \{\mathbf{u}_{j,1}, \mathbf{u}_{j,2}, \mathbf{u}_{j,1} \times \mathbf{u}_{j,2}\}_{j=1}^N \in \mathbb{R}^{3 \times 3}$. Since \mathbf{V}_{out} is rotation equivariant, the constructed frames are also rotation equivariant. We refer to the whole module to generate local frames as Equiv-FrameNet:

$$\mathbf{F}_l \leftarrow \text{Equiv-FrameNet}(c, H_{in}, \mathbf{V}_{in}), \quad (5)$$

where $\mathbf{F}_l = \{\mathbf{F}_j\}_{j=1}^N$ denotes the local frames of each point or joint from the carrier.

Social Affordance Canonicalization. We propose a canonical social affordance canonicalization technique to simplify the distribution. We will explain in detail how to canonicalize social affordance using learned local frame \mathbf{F}_l .

Since we have learned an equivariant local frame \mathbf{F}_l for every point or joint from the carrier, we first transform the motions of the human actor into the frame of each point or joint. Next, we encode the human actor's motions from the perspective of each point to obtain a dense object-centric HOI representation. This can be seen as binding an 'observer' to each point on the object, and each 'observer' en-

codes the actor's motions from a first-person view. The advantage is that it tightly associates the object's motion with the actor's motion, simplifying the distribution of social affordance and facilitating network learning.

Canonical Carrier-centric actor representation. Given a human actor h^i and a carrier c^i at time step i , we define the canonical carrier-centric actor representation R_c^i as:

$$R_c^i(h^i, c^i) = \{(x_j^i, \mathbf{F}_j^i, \epsilon_\theta(h_j^i))\}_{j=1}^N, \quad (6)$$

where \mathbf{F}_j^i is the local frame, h_j^i is the transformed human actor in frame \mathbf{F}_j^i .

Canonical Social Affordance representation. Based upon canonical carrier-centric actor representation R_c^i , we define the canonical social affordance representation A_c^i as:

$$A_c^i = \{R_c^t\}_{t=1}^i = \{ \{(x_j^t, \mathbf{F}_j^t, \epsilon_\theta(h_j^t))\}_{j=1}^N \}_{t=1}^i, \quad (7)$$

where A^i refers to the canonical social affordance representation at time step i and \mathbf{F}_j^i is the local frame.

4.4. Social Affordance Forecasting

Social affordance forecasting is to anticipate human actors' behavior so that the humanoid reactor can provide more reasonable responses. In real situations, the humanoid reactor can only observe the historical motions of the human actor. We believe that the humanoid reactor should have the ability to predict the motions of the human actor in order to better plan its own motions. For example, when someone raises their hand and walks towards you, you might instinctively think they are going to shake hands with you and be prepared for a handshake. Here, we introduce how to enable the reactor to make motion forecasting during prediction.

The t observed motions of human actor and carrier are noted as $\mathbf{s}^{1:M} = [s^1; s^2; \dots; s^M]$. Therefore, the problem

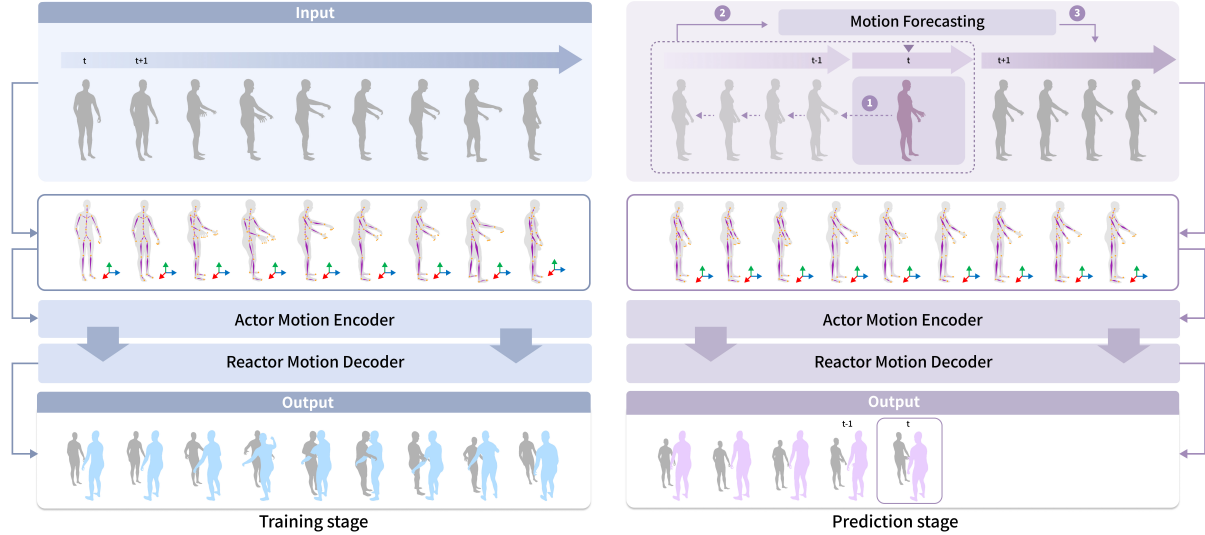


Figure 4. Social Affordance Forecasting. At the training stage, the humanoid reactor can access all motions of the actor. At the prediction stage in the real world, the humanoid reactor can only observe the past motions of the human actor. The forecasting module can anticipate the motions that the human will take.

of online reaction synthesis is modeled as predicting \mathbf{s}_r^M given $\mathbf{s}^{1:M}$. Given the observed motion $\mathbf{s}^{1:M}$, the objective of the motion forecasting problem is to predict the following L motions $\mathbf{s}^{M+1:M+L} = [\mathbf{s}^{M+1}; \mathbf{s}^{M+2}; \dots; \mathbf{s}^{M+L}]$.

We use a motion forecasting module to predict the human actor’s motion and the object’s motion (if available). For human-humanoid interaction setting, we use HumanMAC[10] as the forecasting module. For human-object-humanoid interaction setting, we build our motion forecasting module based on InterDiff[51] and add a prior that human-object contact is stable in order to simplify the difficulty in predicting the object’s motion. Finally, with the predicted result, we can obtain the carrier-centric actor representation $\{R_c^i\}_{i=1}^{M+L} = 1$, we define the canonical complete social affordance representation A_{cf}^i as:

$$A_{cf}^i = \{R_c^t\}_{t=1}^{M+L} = \{ \{ (\mathbf{x}_j^t, \mathbf{F}_j^t, \epsilon_\theta(h_j^t)) \}_{j=1}^N \}_{t=1}^{M+L}, \quad (8)$$

where A_{cf}^i refers to the canonical complete social affordance representation at time step i and F_j^i is the local frame.

4.5. Network and Objective Design

Our network consists of a graph neural network and a 4D Transformer autoencoder. The graph neural network[43] transforms the human actor skeleton into a graph, efficiently modeling the relative motion between different joints. The 4D Transformer autoencoder[48] is composed of a motion encoder and a motion decoder. The motion encoder takes the canonical complete social affordance as input and generates a latent embedding of it. The motion decoder uses the latent embedding as a condition and takes the previously taken motions of the reactor as input to generate new reaction motions autoregressively.

Specifically, given a sequence s , we can compute the A_{cf} , and we can obtain the motions of the reactor s_r by a 4D Transformer network.

$$\hat{s}_r = 4DNet(A_{cf}), \quad (9)$$

where $4DNet$ denotes the whole 4D backbone to generate the motions of humanoid reactor.

We use two loss functions to train our model. The first one is the sequence loss which compares the generated position of joints with the ground truth using the Mean Square Error. The second one is the velocities of each joint.

$$Loss = MSE(s_r - \hat{s}_r) + MSE(ds_r - \hat{d}s_r), \quad (10)$$

where s_r refers to the GT position of each joint and ds_r refers to the velocities of it.

5. Experiments

5.1. Datasets and Metric

CoChair Datasets. We use 2000 sequences of data as the training set and 1000 sequences as the test set. The one initiating the motion is the actor and he/she knows the carrying destination, while the other person is the reactor.

HHI Datasets. We use 3000 sequences of data as the training set and 2000 sequences as the test set. The one initiating the action is the actor, while the other person is the reactor. It includes a total of 30 action categories.

InterHuman Datasets.[30] According to the official splits, we have selected 5200 sequences as the training set and 1177 sequences as the test set. Since there is no obvious initiator of actions in this dataset, we assume that the first person is the actor and the other person is the reactor. The

Method	FID ↓			Diversity →			Accuracy ↑			User Preference↑		
	HHI	InterHuman[30]	Chi3D[17]	HHI	InterHuman[30]	Chi3D[17]	HHI	InterHuman	Chi3D[17]	HHI	InterHuman[30]	Chi3D[17]
Real	0.21	0.17	0.05	10.8	12.4	14.0	88.2	-	80.4	-	-	-
PGBIG[33]	56.7	87.2	67.2	13.9	17.1	17.8	34.1	-	61.6	4.4	1.0	8.3
SS-Transformer[2]	77.8	107.3	54.9	16.2	18.5	19.2	51.9	-	57.1	2.7	4.6	18.4
InterFormer[12]	54.3	73.1	20.8	14.1	14.2	14.8	77.9	-	62.2	6.0	2.1	13.7
InterGen-Revised[30]	19.8	25.7	17.7	11.6	13.3	14.2	80.2	-	71.9	19.7	41.7	15.4
Ours	13.3	14.7	12.8	11.1	13.3	14.1	85.4	-	77.6	67.2	50.6	44.2

Table 2. Quantitative results on HHI, InterHuman, and Chi3D. Our method consistently outperforms the previous method in all metrics.

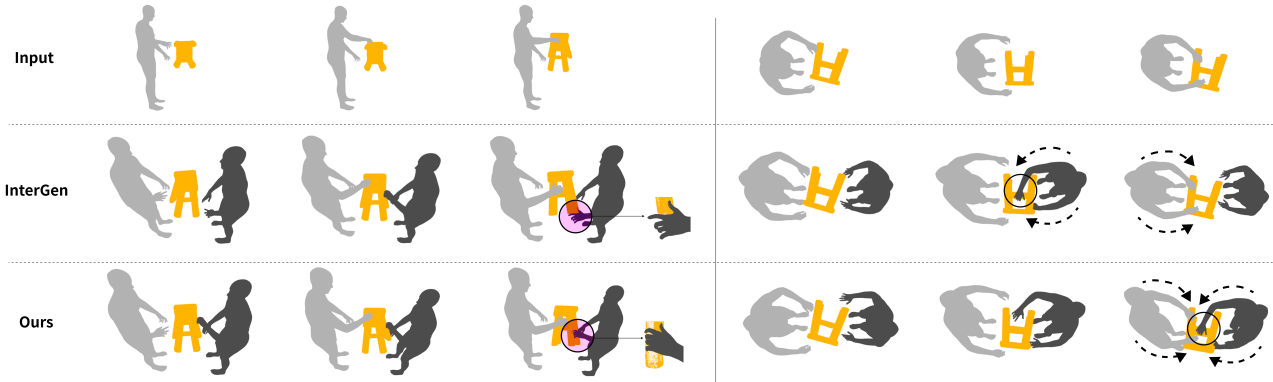


Figure 5. Visualization results on CoChair. Our method can provide a more reasonable grasp and better collaboration with the human actor.

dataset does not have fixed action categories, and each action corresponds to several textual descriptions.

Chi3D Datasets.[17] We have a total of 373 available data provided by officials. Among them, 257 are used as the training set and 116 as the testing set. We consider the person estimated from images as actors and the other one captured by motion capture devices as reactors.

Metrics. We use metrics commonly used in motion generation for quantitative results including action recognition accuracy, Frechet Inception Distance, and diversity. Classification Accuracy measures how well our generated samples are classified by a motion classifier. FID computes the distance between the ground truth and the generated data distribution. Diversity Score is the average deep feature distance between all the samples. For human-object-humanoid setting, we also report the mean penetration depth(cm) when the distance between objects and generated reaction grasps is smaller than 0.2cm, which is commonly used for hand-object interaction[54, 57]. For motion feature extraction, we train an action recognition model using PPtr[48] on each dataset and use it as the motion feature extractor. Due to CoChair and InterHuman not having a clear motion category, we use the feature extractor trained on the HHI dataset. PPtr is a Transformer-based 4D backbone to extract interaction motion features. We generate 1000 samples 10 times with different random seeds.

Method	FID ↓	Diversity →	Penetration depth↓	User Preference↑
Real	0.07	16.4	0.5	-
PGBIG[33]	47.6	14.8	7.2	3.5
SS-Transformer[2]	51.2	15.7	3.7	3.3
InterFormer[12]	44.2	15.5	4.2	6.4
InterGen-Revised[30]	26.7	17.4	2.2	28.0
Ours	7.8	16.9	0.9	58.8

Table 3. Quantitative results on CoChair dataset.

5.2. Baselines

For all baseline methods, we entirely used the author’s code or made some modifications to adapt it to our task.

Progressively Generating Better Initial Guesses[33] uses Spatial Dense Graph Convolutional Networks and Temporal Dense Graph Convolutional Networks.

Spatio-temporal Transformer[2] is a transformer-based architecture that uses attention to find temporal and spatial correlations to predict human motion.

InterFormer[12] consists of a Transformer network with both temporal and spatial attention to capturing the temporal and spatial dependencies of interactions.

InterGen-revised[30] is a powerful diffusion-based framework that can generate multi-human interaction based on the text description. We replace the CLIP branch with a spatio-temporal transformer to encode the actor’s motion.

5.3. Comparison to State-of-the-arts

The results on the CoChair dataset are shown in Tab 3. Our method consistently outperforms previous method in all metrics. We compared the results with InterHuman

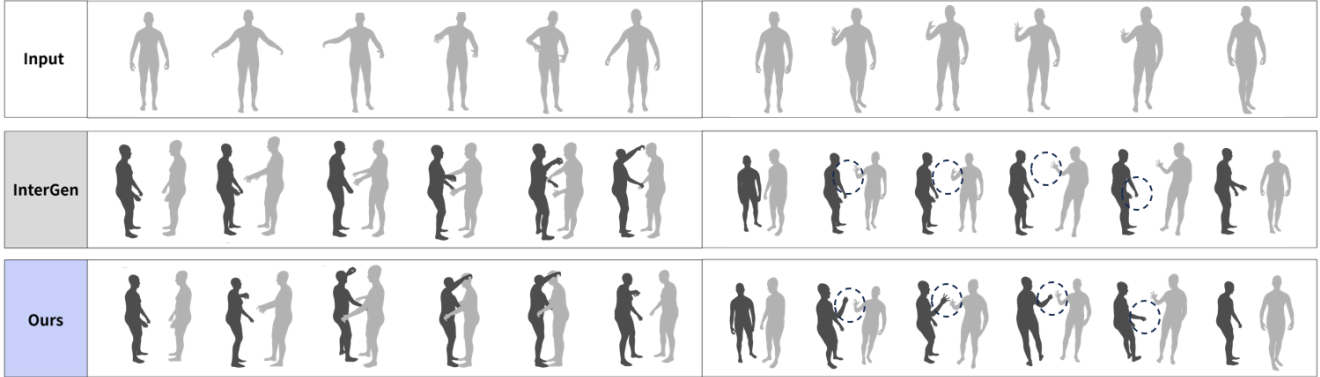


Figure 6. Visualization results on HHI. Our method can generate more prompt reactions and can better capture hand motion.



Figure 7. Visualization gallery of our method on InterHuman (left) and Chi3D(right). The deep black one is generated by our method.

and Fig 5, and it can be seen that our method can generate a more realistic and natural grasp(left) and collaboration(right). This indicates that through social affordance canonicalization, our approach can simplify the feature space, thus generating more complex and delicate motions. Through social affordance forecasting, we can anticipate the motions of human actors, thereby better planning cooperation with humans. As for the human-humanoid interaction setting, the results are shown in Tab 2, our method outperforms baselines in all metrics. Some visualization results are shown in Fig 6. Compared with InterGen, our method can generate prompt reaction(left), and can better capture the local hand motions(right), while InterGen fails. We show that our method still can outperform the state-of-the-art method on existing human-human interaction datasets. We show the visualization results on InterHuman and Chi3D as shown in Fig 7, results demonstrate that our method generates a wide variety of realistic reactions.

5.4. Ablation and Discussion

Ablation Study. To validate our method, we conducted ablation experiments on the HHI dataset to verify the effectiveness of each design. Without canonicalization, our method drops significantly, indicating that the use of social affordance canonicalization to simplify feature space complexity is essential. Without social affordance forecasting, our

method lost the ability to predict human actor motions, also leading to a performance drop. To verify the necessity of using the local frame, we also compared the effect of using a global frame, and it can be seen that our method is significantly superior. This also indicates that using a local frame to describe local geometry and potential contact is valuable.

Method	FID ↓	Diversity →	Accuracy ↑	User Preference ↑
Real	0.21	10.8	88.2	-
wo canonicalization	34.5	12.5	78.4	13.4
wo forecasting	16.7	11.4	82.1	19.4
w global frame	28.4	8.9	79.6	20.1
Ours	13.3	11.1	85.4	47.1

Table 4. Ablation study to justify each design of our method.

Visualization of Learned Local Frame for Carrier. We visualized the frames on the rest-posed humanoid carrier. It can be seen that the frames on the spine are basically consistent, and the joint frames on the left and right sides exhibit roughly symmetrical characteristics. We also visualize the local frames, and it can be seen that the frames on the chair legs are approximately the same and can be generalized to different chairs.

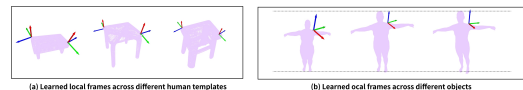


Figure 8. Visualization results of learned local frame. The local frames are roughly consistent across different chairs.

Visualization of Motion Forecasting. We visualized the results of motion forecasting, and it can be seen that our method can provide reasonable predictions of whether there are objects or not. The imagination of these future behaviors can help the humanoid reactor to give more prompt and reasonable reactions.

Computation Overhead. We computed the computational overhead of our method and compared it with InterGen[30]. All tests were conducted on a single 80G A100 graphics card. We set the input action sequence to 250 frames. In



Figure 9. Visualization results of Motion Forecasting with object(left) and without object(right).

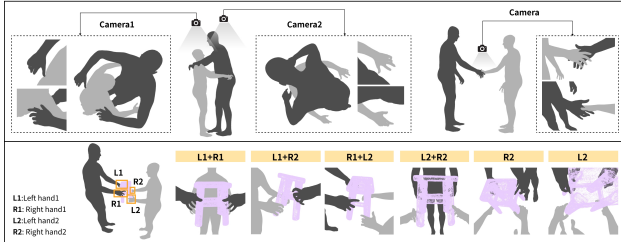


Figure 10. The Quality of Our Datasets.

terms of the number of parameters, our method is significantly more lightweight. The proposed social affordance canonicalization simplifies the distribution of actor motions, thus reducing the need for a large number of network parameters. Moreover, our method nearly achieves real-time inference at approximately 25 fps, whereas InterGen only reaches 0.54 fps. It’s worth mentioning that our proposed FrameNet, utilizing merely 122 B of parameters, accomplishes the canonicalization of social affordance. Results show that our method has great potential and application in the fields of AR/VR games and humanoid robot control.

Method	Memory	Parameter	FPS
InterGen-Revised[30]	38.12G	291.29M	0.54fps
Ours	22.28G	11.70M	25fps

Table 5. Our method is significantly more lightweight and can achieve real-time inference at approximately 25 FPS.

The Quality of Our Datasets. Our motion capture system has a high accuracy of 0.019 mm, effectively capturing contact regions as demonstrated in the figures below. We have thoroughly inspected the dataset to ensure its quality.

6. Conclusions

We propose a new task named online full-body motion reaction synthesis, which generates humanoid reactions based on the human actor’s motions. We construct two datasets to support the research on the reaction synthesis task, HHI for Human-Humanoid Interaction and CoChair for Human-Object-Humanoid Interaction. We propose a novel technique named social affordance canonicalization and forecasting to achieve realistic and natural humanoid reaction synthesis. Experiments demonstrate that our approach can effectively generate high-quality reactions on proposed datasets and existing datasets.

References

- [1] Chaitanya Ahuja and Louis-Philippe Morency. Language2pose: Natural language grounded pose forecasting. In *2019 International Conference on 3D Vision (3DV)*, pages 719–728. IEEE, 2019. 2
- [2] Emre Aksan, Manuel Kaufmann, Peng Cao, and Otmar Hilliges. A spatio-temporal transformer for 3d human motion prediction. In *2021 International Conference on 3D Vision (3DV)*, pages 565–574. IEEE, 2021. 7
- [3] Sadegh Aliakbarian, Fatemeh Sadat Saleh, Mathieu Salzmann, Lars Petersson, and Stephen Gould. A stochastic conditioning scheme for diverse human motion prediction. In *CVPR*, pages 5223–5232, 2020. 2
- [4] Nikos Athanasiou, Mathis Petrovich, Michael J Black, and Gül Varol. Teach: Temporal action composition for 3d humans. In *2022 International Conference on 3D Vision (3DV)*, pages 414–423. IEEE, 2022. 1, 2
- [5] Murchana Baruah and Bonny Banerjee. A multimodal predictive agent model for human interaction generation. In *Proceedings of the IEEE/CVF conference on computer vision and pattern recognition workshops*, pages 1022–1023, 2020. 3
- [6] Murchana Baruah, Bonny Banerjee, and Atulya K Nagar. Intent prediction in human–human interactions. *IEEE Transactions on Human-Machine Systems*, 53(2):458–463, 2023. 2
- [7] Andreas Blattmann, Timo Milbich, Michael Dorkenwald, and Bjorn Ommer. Behavior-driven synthesis of human dynamics. In *CVPR*, pages 12236–12246, 2021. 2
- [8] Arij Bouazizi, Adrian Holzbock, Ulrich Kressel, Klaus Dietmayer, and Vasileios Belagiannis. Motionmixer: Mlp-based 3d human body pose forecasting. In *IJCAI*, 2022. 2
- [9] Pablo Cervantes, Yusuke Sekikawa, Ikuro Sato, and Koichi Shinoda. Implicit neural representations for variable length human motion generation. In *European Conference on Computer Vision*, pages 356–372. Springer, 2022. 2
- [10] Ling-Hao Chen, Jiawei Zhang, Yewen Li, Yiren Pang, Xiaobo Xia, and Tongliang Liu. Humanmac: Masked motion completion for human motion prediction. *arXiv preprint arXiv:2302.03665*, 2023. 2, 6
- [11] Xin Chen, Biao Jiang, Wen Liu, Zilong Huang, Bin Fu, Tao Chen, and Gang Yu. Executing your commands via motion diffusion in latent space. In *Proceedings of the IEEE/CVF Conference on Computer Vision and Pattern Recognition*, pages 18000–18010, 2023. 2
- [12] Baptiste Chopin, Hao Tang, Naima Otberdout, Mohamed Daoudi, and Nicu Sebe. Interaction transformer for human reaction generation. *IEEE Transactions on Multimedia*, 2023. 2, 7
- [13] Sammy Christen, Muhammed Kocabas, Emre Aksan, Jemin Hwangbo, Jie Song, and Otmar Hilliges. D-grasp: Physically plausible dynamic grasp synthesis for hand-object interactions. In *Proceedings of the IEEE/CVF Conference on Computer Vision and Pattern Recognition*, pages 20577–20586, 2022. 1
- [14] Enric Corona, Albert Pumarola, Guillem Alenyà, and

- Francesc Moreno-Noguer. Context-aware human motion prediction. In *CVPR*, 2020. 2
- [15] Rishabh Dabral, Muhammad Hamza Mughal, Vladislav Golyanik, and Christian Theobalt. Mofusion: A framework for denoising-diffusion-based motion synthesis. In *Proceedings of the IEEE/CVF Conference on Computer Vision and Pattern Recognition*, pages 9760–9770, 2023. 1, 2
- [16] Lingwei Dang, Yongwei Nie, Chengjiang Long, Qing Zhang, and Guiqing Li. Diverse human motion prediction via gumbel-softmax sampling from an auxiliary space. In *ACM MM*, pages 5162–5171, 2022. 2
- [17] Mihai Fieraru, Mihai Zanfir, Elisabeta Oneata, Alin-Ionut Popa, Vlad Olaru, and Cristian Sminchisescu. Three-dimensional reconstruction of human interactions. In *Proceedings of the IEEE/CVF Conference on Computer Vision and Pattern Recognition*, pages 7214–7223, 2020. 3, 7
- [18] Chuan Guo, Xinxin Zuo, Sen Wang, Shihao Zou, Qingyao Sun, Annan Deng, Minglun Gong, and Li Cheng. Action2motion: Conditioned generation of 3d human motions. In *Proceedings of the 28th ACM International Conference on Multimedia*, pages 2021–2029, 2020. 1, 2
- [19] Chuan Guo, Shihao Zou, Xinxin Zuo, Sen Wang, Wei Ji, Xingyu Li, and Li Cheng. Generating diverse and natural 3d human motions from text. In *Proceedings of the IEEE/CVF Conference on Computer Vision and Pattern Recognition*, pages 5152–5161, 2022. 2
- [20] Agrim Gupta, Justin Johnson, Li Fei-Fei, Silvio Savarese, and Alexandre Alahi. Social gan: Socially acceptable trajectories with generative adversarial networks. In *CVPR*, pages 2255–2264, 2018. 2
- [21] Alejandro Hernandez, Jurgen Gall, and Francesc Moreno-Noguer. Human motion prediction via spatio-temporal inpainting. In *Proceedings of the IEEE/CVF International Conference on Computer Vision*, pages 7134–7143, 2019. 2
- [22] Biao Jiang, Xin Chen, Wen Liu, Jingyi Yu, Gang Yu, and Tao Chen. Motiongpt: Human motion as a foreign language. *arXiv preprint arXiv:2306.14795*, 2023. 1, 2
- [23] Bowen Jing, Stephan Eismann, Patricia Suriana, Raphael JL Townshend, and Ron Dror. Learning from protein structure with geometric vector perceptrons. *arXiv preprint arXiv:2009.01411*, 2020. 4, 5
- [24] Jihoon Kim, Jiseob Kim, and Sungjoon Choi. Flame: Free-form language-based motion synthesis & editing. In *Proceedings of the AAAI Conference on Artificial Intelligence*, pages 8255–8263, 2023. 2
- [25] Hsin-Ying Lee, Xiaodong Yang, Ming-Yu Liu, Ting-Chun Wang, Yu-Ding Lu, Ming-Hsuan Yang, and Jan Kautz. Dancing to music. *Advances in neural information processing systems*, 32, 2019. 2
- [26] Namhoon Lee, Wongun Choi, Paul Vernaza, Christopher B Choy, Philip HS Torr, and Manmohan Chandraker. Desire: Distant future prediction in dynamic scenes with interacting agents. In *CVPR*, pages 336–345, 2017. 2
- [27] Buyu Li, Yongchi Zhao, Shi Zhelun, and Lu Sheng. Danceformer: Music conditioned 3d dance generation with parametric motion transformer. In *Proceedings of the AAAI Conference on Artificial Intelligence*, pages 1272–1279, 2022. 2
- [28] Chen Li, Zhen Zhang, Wee Sun Lee, and Gim Hee Lee. Convolutional sequence to sequence model for human dynamics. In *CVPR*, pages 5226–5234, 2018. 2
- [29] Ruilong Li, Shan Yang, David A Ross, and Angjoo Kanazawa. Ai choreographer: Music conditioned 3d dance generation with aist++. In *Proceedings of the IEEE/CVF International Conference on Computer Vision*, pages 13401–13412, 2021. 2
- [30] Han Liang, Wenqian Zhang, Wenxuan Li, Jingyi Yu, and Lan Xu. Intergen: Diffusion-based multi-human motion generation under complex interactions. *arXiv preprint arXiv:2304.05684*, 2023. 1, 2, 3, 6, 7, 8, 9
- [31] Jun Liu, Amir Shahroudy, Mauricio Perez, Gang Wang, Ling-Yu Duan, and Alex C Kot. Ntu rgb+ d 120: A large-scale benchmark for 3d human activity understanding. *IEEE transactions on pattern analysis and machine intelligence*, 42(10):2684–2701, 2019. 3
- [32] Thomas Lucas, Fabien Baradel, Philippe Weinzaepfel, and Grégory Rogez. Posegpt: quantization-based 3d human motion generation and forecasting. In *ECCV*, 2022. 2
- [33] Tiezheng Ma, Yongwei Nie, Chengjiang Long, Qing Zhang, and Guiqing Li. Progressively generating better initial guesses towards next stages for high-quality human motion prediction. In *Proceedings of the IEEE/CVF Conference on Computer Vision and Pattern Recognition*, pages 6437–6446, 2022. 7
- [34] Naureen Mahmood, Nima Ghorbani, Nikolaus F Troje, Gerard Pons-Moll, and Michael J Black. Amass: Archive of motion capture as surface shapes. In *ICCV*, 2019. 4
- [35] Wei Mao, Miaomiao Liu, Mathieu Salzmann, and Hongdong Li. Learning trajectory dependencies for human motion prediction. In *ICCV*, pages 9489–9497, 2019. 2
- [36] Julieta Martinez, Michael J Black, and Javier Romero. On human motion prediction using recurrent neural networks. In *CVPR*, pages 2891–2900, 2017. 2
- [37] Evonne Ng, Donglai Xiang, Hanbyul Joo, and Kristen Grauman. You2me: Inferring body pose in egocentric video via first and second person interactions. In *Proceedings of the IEEE/CVF Conference on Computer Vision and Pattern Recognition*, pages 9890–9900, 2020. 3
- [38] Georgios Pavlakos, Vasileios Choutas, Nima Ghorbani, Timo Bolkart, Ahmed AA Osman, Dimitrios Tzionas, and Michael J Black. Expressive body capture: 3d hands, face, and body from a single image. In *Proceedings of the IEEE/CVF conference on computer vision and pattern recognition*, pages 10975–10985, 2019. 4
- [39] Mathis Petrovich, Michael J Black, and Gül Varol. Action-conditioned 3d human motion synthesis with transformer vae. In *Proceedings of the IEEE/CVF International Conference on Computer Vision*, pages 10985–10995, 2021. 2
- [40] Mathis Petrovich, Michael J Black, and Gül Varol. Temos: Generating diverse human motions from textual descriptions. In *European Conference on Computer Vision*, pages 480–497. Springer, 2022. 1, 2
- [41] Alec Radford, Jong Wook Kim, Chris Hallacy, Aditya Ramesh, Gabriel Goh, Sandhini Agarwal, Girish Sastry, Amanda Askell, Pamela Mishkin, Jack Clark, et al. Learning

- transferable visual models from natural language supervision. In *International conference on machine learning*, pages 8748–8763. PMLR, 2021. 2
- [42] Tim Salzman, Marco Pavone, and Markus Ryll. Motron: Multimodal probabilistic human motion forecasting. In *CVPR*, pages 6457–6466, 2022. 2
- [43] Franco Scarselli, Marco Gori, Ah Chung Tsoi, Markus Hagenbuchner, and Gabriele Monfardini. The graph neural network model. *IEEE transactions on neural networks*, 20(1): 61–80, 2008. 6
- [44] Yonatan Shafir, Guy Tevet, Roy Kapon, and Amit H Bermano. Human motion diffusion as a generative prior. *arXiv preprint arXiv:2303.01418*, 2023. 2
- [45] Theodoros Sofianos, Alessio Sampieri, Luca Franco, and Fabio Galasso. Space-time-separable graph convolutional network for pose forecasting. In *ICCV*, 2021. 2
- [46] Sebastian Starke, Yiwei Zhao, Taku Komura, and Kazi Zaman. Local motion phases for learning multi-contact character movements. *ACM Transactions on Graphics (TOG)*, 39(4):54–1, 2020. 2
- [47] Yongyi Tang, Lin Ma, Wei Liu, and Wei-Shi Zheng. Long-term human motion prediction by modeling motion context and enhancing motion dynamic. In *IJCAI*, 2018. 2
- [48] Hao Wen, Yunze Liu, Jingwei Huang, Bo Duan, and Li Yi. Point primitive transformer for long-term 4d point cloud video understanding. In *European Conference on Computer Vision*, pages 19–35. Springer, 2022. 6, 7
- [49] Liang Xu, Ziyang Song, Dongliang Wang, Jing Su, Zhicheng Fang, Chenjing Ding, Weihao Gan, Yichao Yan, Xin Jin, Xiaokang Yang, et al. Actformer: A gan-based transformer towards general action-conditioned 3d human motion generation. In *Proceedings of the IEEE/CVF International Conference on Computer Vision*, pages 2228–2238, 2023. 1, 2
- [50] Sirui Xu, Yu-Xiong Wang, and Liang-Yan Gui. Diverse human motion prediction guided by multi-level spatial-temporal anchors. In *ECCV*, 2022. 2
- [51] Sirui Xu, Zhengyuan Li, Yu-Xiong Wang, and Liang-Yan Gui. Interdiff: Generating 3d human-object interactions with physics-informed diffusion. In *Proceedings of the IEEE/CVF International Conference on Computer Vision*, pages 14928–14940, 2023. 1, 2, 6
- [52] Sijie Yan, Zhizhong Li, Yuanjun Xiong, Huahan Yan, and Dahua Lin. Convolutional sequence generation for skeleton-based action synthesis. In *Proceedings of the IEEE/CVF International Conference on Computer Vision*, pages 4394–4402, 2019. 2
- [53] Kiwon Yun, Jean Honorio, Debaleena Chattopadhyay, Tamara L Berg, and Dimitris Samaras. Two-person interaction detection using body-pose features and multiple instance learning. In *2012 IEEE computer society conference on computer vision and pattern recognition workshops*, pages 28–35. IEEE, 2012. 3
- [54] He Zhang, Yuting Ye, Takaaki Shiratori, and Taku Komura. Manipnet: neural manipulation synthesis with a hand-object spatial representation. *ACM Transactions on Graphics (TOG)*, 40(4):1–14, 2021. 1, 7
- [55] Hui Zhang, Sammy Christen, Zicong Fan, Luocheng Zheng, Jemin Hwangbo, Jie Song, and Otmar Hilliges. Artigrasp: Physically plausible synthesis of bi-manual dexterous grasping and articulation. *arXiv preprint arXiv:2309.03891*, 2023. 1
- [56] Mingyuan Zhang, Zhongang Cai, Liang Pan, Fangzhou Hong, Xinying Guo, Lei Yang, and Ziwei Liu. Motiondiffuse: Text-driven human motion generation with diffusion model. *arXiv preprint arXiv:2208.15001*, 2022. 1, 2
- [57] Juntian Zheng, Qingyuan Zheng, Lixing Fang, Yun Liu, and Li Yi. Cams: Canonicalized manipulation spaces for category-level functional hand-object manipulation synthesis. In *Proceedings of the IEEE/CVF Conference on Computer Vision and Pattern Recognition*, pages 585–594, 2023. 1, 7
- [58] Chongyang Zhong, Lei Hu, Zihao Zhang, Yongjing Ye, and Shihong Xia. Spatio-temporal gating-adjacency gen for human motion prediction. In *CVPR*, 2022. 2
- [59] Tianqiang Zhu, Rina Wu, Xiangbo Lin, and Yi Sun. Toward human-like grasp: Dexterous grasping via semantic representation of object-hand. In *Proceedings of the IEEE/CVF International Conference on Computer Vision*, pages 15741–15751, 2021. 1